# Electrical conductivity of carbon plasma

Alan W. DeSilva
*Institute for Research in Electronics and Applied Physics, University of Maryland, College Park, Maryland 20742, USA*

G. B. Vunni
*U. S. Army Research Laboratory, Aberdeen Proving Ground, Maryland 20005, USA*

(Received 28 October 2008; published 13 March 2009)

The electrical conductivity of carbon plasmas is measured in the range of densities from about 0.6 solid density down to about 0.05 solid density, and reported for values of internal energy ranging from 2 to 22 kJ/gm. Plasmas are formed by rapid electrical discharge through thin graphite fibers immersed in a water bath. The pressure in the expanding plasma column is determined by use of a hydrodynamic model to describe the effect on the water surround. It is found that at constant internal energy per unit mass $U$, conductivity $\sigma$ varies with specific volume $v$ as $\sigma = v^{-\alpha}$, where $\alpha$ is about 1 for $U < 6$ kJ/gm, and rises to about 1.5 for $U = 22$ kJ/gm.

DOI: 10.1103/PhysRevE.79.036403 PACS number(s): 52.25.Fi, 52.80.Qj, 52.27.Gr

## I. INTRODUCTION

Electrical conductivity of plasmas formed of nonmetals might be expected to show different characteristics from those of pure metal plasmas. Carbon is such a nonmetal in its normal state as graphite. Measurements of resistivity and specific heat of graphite reported in the literature show wide variations depending on the sample preparation and configuration. Since graphite electrodes are in wide use, and carbon plasmas form necessarily whenever an arc is struck with such an electrode, a study of carbon conductivity may be of industrial, as well as of basic scientific interest. Although the conductivity of dense metal plasmas has been extensively studied and reported [1–10] the conductivity of carbon in the plasma state has received less attention [11,12], perhaps owing to the difficulty in preparing plasmas of carbon for study. In this paper, we report results of measurement of the electrical conductivity of 94% pure carbon plasma for densities ranging from about 60% of solid density, down to about 1% of solid density.

In work reported previously by one of us (A.W.D., Refs. [1,2]), the electrical conductivity of dense metal plasmas was measured over densities ranging from near solid density down to abut 1% of solid density. These measurements were made in plasmas created by rapid heating and vaporization of a wire sample in a water bath, and yielded the conductivity as a function of density and temperature. The pressure and temperature were determined with aid of the SESAME tabulated equation of state tables obtained from the Los Alamos National Laboratory [13]. In this paper we report the use of the same method to create more or less pure carbon plasmas and to measure their conductivity. However, the conductivity results reported in this work do not depend the use of tabulated equation of state tables, and the data are presented as functions of internal energy and specific volume.

## II. EXPERIMENT

For this study, we were unable to find a source for solid pure carbon rods smaller than 2 mm diameter. The energy available in our capacitor bank is insufficient to vaporize such thick rods.Therefore the form of carbon utilized in this study is a bundle of fine graphite fibers termed a "tow," by the industry. The individual fibers are derived from a thread of polymerized acrylonitrile (PAN) that has been oxidized and then baked at a high temperature "graphitized" which turns it into nearly pure carbon. Such tows are intended for a number of uses where light strong composite materials are desired. The tow used in this work was supplied by the Hex-Cel Corporation, designated "AS4C-GP," and consists of a bundle of 3000 fine graphite fibers, each 6.9 $\mu$ in diameter, bound together with a small amount of sizing. The carbon content of the fibers is given by the manufacturer as 94%, with the remainder being nitrogen with trace amounts of sodium and silicon. The mass per unit length of the tow is 0.191 gm/m, and using the total cross sectional area occupied by fibers, we find the graphite density is 1.70 gm/cc, compared with 2.25 gm/cc density of single crystal graphite [11]. As supplied, the bundle has a flat rectangular cross section measuring 1.49 mm in width and 0.12 mm in thickness, yielding a cross-sectional area of 0.178 $mm^2$, compared to the area obtained by summing the 3000 individual fiber cross sections, which gives a total of 0.112 $mm^2$. Therefore the fraction of the cross-sectional area occupied by carbon fiber in the tow is 63%, and so the effective initial density of carbon is 1.073 gm/cc. Note that geometrically, 62% is the result of close hexagonal packing of the individual fibers. The tow used in this study has resistance 1.3 Ohm/cm, which leads to a room temperature conductivity for the graphite of which the fibers are made of $6.86 \times 10^4$ Siemens/m.

Measurements are made in a cylindrical aluminum chamber 30 cm in diameter and 15 cm deep (Fig. 1). The fiber sample is clamped between an active electrode in the center of the chamber, and to a return electrode above, and has an overall length of 15 mm, and resistance 2.1 Ohms. In order to provide effective cylindrical symmetry, before being clamped at the top electrode, the flat fiber is twisted through about three turns, to form a nearly round bundle approximately 0.48 mm in diameter. The chamber is then filled with water. The fiber is rapidly heated and vaporized by current

 

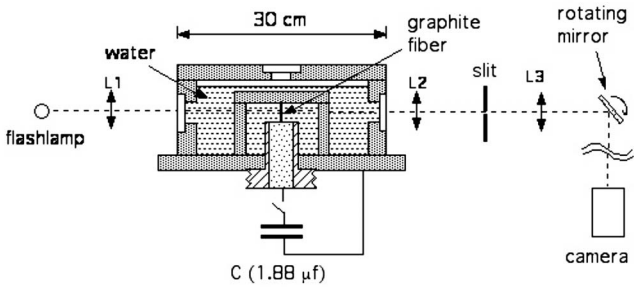


FIG. 1. Schematic diagram of discharge chamber. Lens L1 focusses the flashlamp at the fiber position, L2 focusses the fiber/plasma on the slit, and L3 focusses the light passing through the slit on the camera.

switched into it from a 1.88 $\mu$F capacitor, which may be charged to an initial voltage up to 20 kV. Vaporization occurs in about one microsecond, and as the plasma so formed expands, the water serves to impede the expansion, so that a relatively uniform cylindrical plasma column exists within the plasma-water boundary. In previous work with metal plasmas, we have determined that the assumption that the plasma conditions within the boundary formed by the plasma-water interface are uniform is a good approximation. This follows from the observation that sound speed within the plasma is greater than the boundary expansion speed, so conditions within the boundaries may equalize rapidly.

## III. DIAGNOSTICS

The voltage between the fiber ends is measured with a 670:1 high voltage resistive divider, followed by a 25:1 further divider at the recording digital oscilloscope, with correction made in software for the small reactive component. Current is measured with a Rogowski loop that surrounds the active electrode inside the chamber, the output of which is passively integrated with an RC integrator, and corrected in the analysis software for the slight error owing to the finite RC decay time. The rate of expansion of the plasma column is recorded with aid of a rotating mirror streak camera. The plasma is backlighted by a xenon flashlamp, and imaged on a narrow slit with the plasma axis perpendicular to the slit. The light passing through the slit represents a thin slice across the column diameter at about midway between the electrodes. Light from the slit passes to a rapidly rotating mirror, and is then focused on a digital camera (Fig. 1). The result is an image showing the time history of the plasma column diameter in silhouette (Fig. 2), The plasma-water interface is quite sharply defined for the first several microseconds, as shown by the streak camera images. A spatial reference on the image is provided by a pair of very thin wires stretched across the slit, which appear as a pair of dark lines on the image. A time reference is provided by a pair of spark gaps positioned just in front of the slit (that is, on the flashlamp side), that yield a pair of light spots on the image when fired at preselected times.

The temperature of the plasma-water interface is determined by measurement of the absolute intensity of radiation. Observations made at several wavelengths in the visible indicate that the radiation spectrum is Planckian, so a measurement at any wavelength can serve to give a temperature profile in time. Light from a portion of the plasma column near the midplane is focussed on the entrance slit of a 1/4 m JA monochromator, equipped with 25 mm slits, making it sensitive to a wavelength band about 0.09 nm wide. The entrance slit is masked to about one mm long, and imaging is 1-1, so the portion of the plasma column viewed by the monochromator is restricted to one mm along the column axis near the midplane, and narrow compared to the plasma diameter. The system has been absolutely calibrated with a tungsten striplamp. Observation of Planckian radiation implies that the optical depth of the emitting region is small, so the measurement reveals only a surface temperature in the boundary region between plasma and the surrounding water.

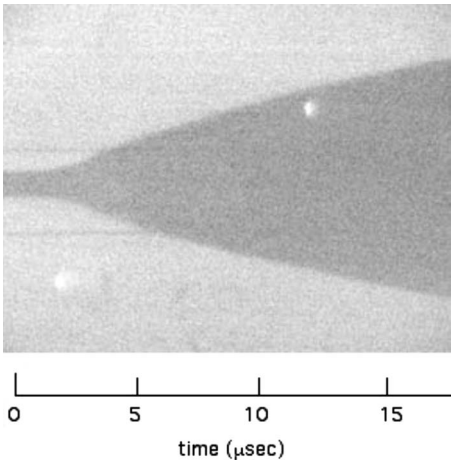


FIG. 2. Streak image of a typical discharge (carc22). Timescale is determined from the two spots of light, occurring at 2.54 and 13.57 $\mu$s after initiation of the discharge. The two horizontal lines are references 1.56 mm apart. Time zero is at initiation of current flow.

## IV. ANALYSIS

The primary recorded data are the voltage and current recorded at four nanosecond intervals, and the column diameter measured from the streak image. The streak images are digitized to give column diameter as a function of time, and the measurements from the images are interpolated to produce a table of plasma diameter at the same 4-ns intervals. The current, voltage, and diameter data are input to an analysis program which steps through these data, tracking the development of column diameter, density, internal energy, and pressure (Fig. 3). A Lagrangian hydrodynamic model for the water relates the measured rate of radial expansion of the column to the pressure at the plasma-water interface. The numerical code used was adapted from Plooster [14], with the equation of state for water taken from Rice and Walsh [15]. The change in internal energy of the plasma in a single four-nanosecond step is then the electrical energy input less the expansion energy $VIdt-pdV$, where it is assumed that the pressure at the interface is equal to the pressure throughout the plasma column. The contribution of 6% nitrogen in the

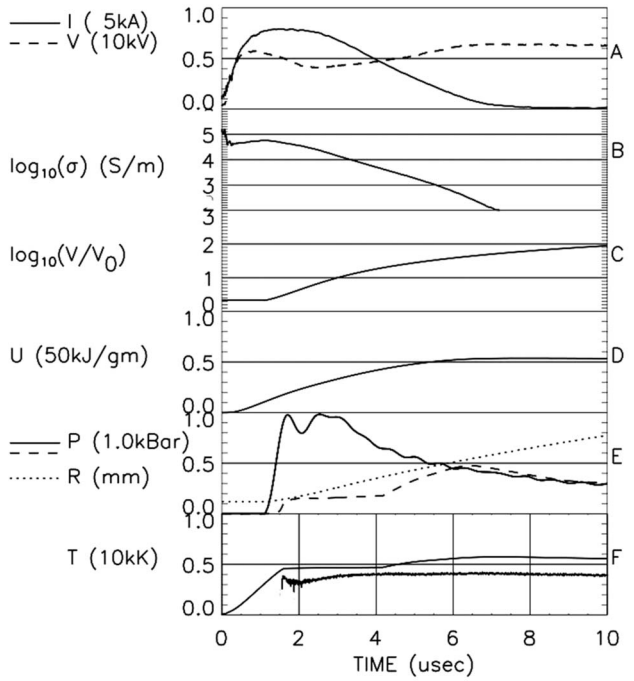


FIG. 3. Time record of the shot pictured in Fig. 2. For this shot the discharge circuit included two Ohms additional resistance, and the the capacitor bank was charged to 16 kV. Scale multipliers and units are shown at left. Measured parameters are the voltage and current and the column radius. All other curves are the result of calculation. A: Voltage and current. B: Conductivity (MKS units). C: Ratio of specific volume to that of solid graphite. D: Internal energy. E: Solid line is pressure from the hydrodynamic model for water, dashed line is the pressure from SESAME, and the dotted line is the measured plasma column radius. F: The thin solid line is temperature from SESAME, and the darker, noisy line is radiation temperature. For temperatures less than about 3500 K, the radiation signal drops into background noise, and has been eliminated from the figure.

fiber composition would have only sbout a 3% effect on the expansion rate of the plasma column, and ionizing the 6% nitrogen would cost about an additional 4% energy over that for pure carbon. Corrections for these effects have been made in the analysis. The column resistance $R$ at each step is simply $V/I$, and the conductivity is then $l/RA$, where $A$ is the instantaneous cross sectional area of the column, and $l$ its length, which is constant due to the massive electrodes. Following this analysis, we search through the data, and select out for plotting those times when the internal energy is within a small range about some pre-selected value. In order to obtain data for a wide range of conditions, we may vary the series reactance in the external circuit and/or the voltage of the capacitor bank on successive discharges. Assembling such data from a large number of shots, we build up a picture of conductivity versus density (or specific volume) and internal energy.

The analysis given above differs from that used in our former work with metal samples, in which the SESAME equation of state database was a necessary part of the analysis. Using the present technique, we do not require the use of a tabulated equation of state database to obtain the conductivity, but use it only to give an independent reading of the pressure and temperature.

## V. RESULTS AND DISCUSSION

Figure 3 shows the result of the analysis on a typical discharge, in this case with a 2 Ohm resistor in series with the capacitor bank, and the bank charged to 16 kV. The measured data are the voltage and current, in window $A$, and the column radius taken from the streak image, shown in window $E$. The rest of the curves are the result of our analysis program, and include the plasma pressure, internal energy, specific volume, and conductivity.

The time history shown in Fig. 3 is typical, and shows that as the plasma expands, the column becomes nonconducting when the internal energy has risen to about 27 kJ/gm, and the plasma volume has increased by a factor of about 40. If the current is increased by either reducing the series resistance in the circuit, or by starting with a higher voltage on the capacitor bank, the column may become nonconducting rather suddenly, but that point still is still associated with internal energy of about 25 kJ/gm.

The pressure deduced from the hydrodynamic model for water is shown in window $E$. Radiation temperature is shown in window $F$. It is of interest to compare these measurements with predictions of the equation of state for carbon in the SESAME database "a7830" [15]. We insert our measurements for density and internal energy into the SESAME table, and note the corresponding pressure and temperature. The temperature deduced from the SESAME database is shown as a solid line in Fig. 3(f). The lack of agreement is probably due to the fact that the radiation temperature measures only the surface temperature, and the SESAME result refers to the bulk property. The flat $T$ vs time SESAME result up to about 4 ms seems to indicate that the SESAME table treats this as a classic vaporization at constant pressure.

The pressure from SESAME is shown in Fig. 3(e), and compared to that determined from the hydrodynamics of the water. The SESAME result for early times, up to the time the plasma has expanded by about a factor ten, are considerably lower than the hydrodynamic result. The pressure determined from the expansion rate of the plasma into the water comes from a straightforward dynamical model, that has been shown to work well in previous work with metal wire explosions. A possible explanation for the discrepancy is that the fibers heat non-uniformly, and that partial vaporization occurs before the bulk of the fibers are heated to the vaporization temperature.

Figure 4 shows the conductivity of carbon plasmas as a function of specific volume, at values of the internal energy ranging from 2 to 22 kJ/gm. At the lowest values of internal energy shown, there has been little expansion of the column, the specific volume remains near its initial value, and the conductivity remains near to the initial value of $6.86 \times 10^4$ Siemens/m. As the plasma absorbs energy, the pressure increases, and the column expands rapidly. Taking the results of a large number of discharges under various initial conditions, we observe that at constant energy, the conductivity diminishes as specific volume increases, the relation-

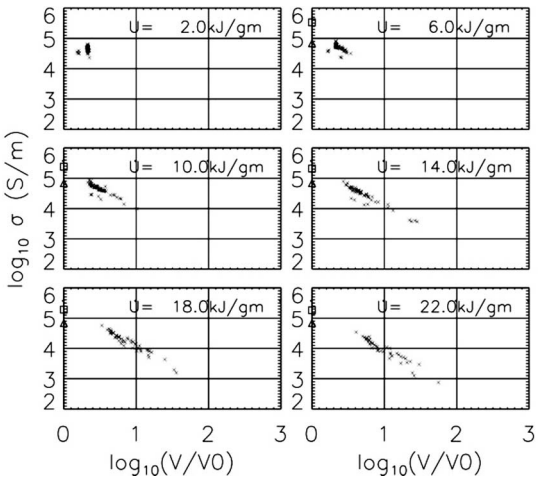


FIG. 4. Conductivity vs specific volume, at six different values of the internal energy density. The triangle symbols at $\log_{10}(V/V0)=0$ are the conductivity of the cold fibers, and the square symbols are data from Ref. [11].

ship approximated by $\sigma=(V/V_0)^{\alpha}$. At 2 kJ/gm, $\alpha$ is approximately unity. As the internal energy increases, the exponent grows to about 1.5 at $U=22$ kJ/gm. At higher values of internal energy, it does not appear to be possible to make a meaningful linear fit to the $\log_{10}(V)-\log_{10}(\sigma)$ data.

At these higher values of internal energy, it has proved impossible to obtain data for $V/V_0$ close to unity. This is because the energy input is not sufficiently fast for the plasma to arrive at high energy before significant expansion occurs. For comparison, we have included in Fig. 4 some data from Korobenko *et al.* [11], in which films of grain-oriented graphite of initial density 2.25 gm/cc were constrained to nearly constant density by being sandwiched between glass slabs during rapid heating. These data seem to fit nicely in the pattern of our data.

Conductivity of carbon plasmas formed by explosions of thin carbon fibers constrained by glass capillaries has also been reported by Haun *et al.* [12]. These results are reported as functions of temperature in the range 9–16 kK, and $V/V_0$ in the range 1 to 2. Our data are in terms of internal energy and specific volume, so in order to compare, we need to appeal to the SESAME tables to find the energy densities associated with the temperatures in Ref. [12]. The EOS tables indicate that over their whole range of reported temperatures and densities, the internal energies are greater than 50 kJ/gm, well above the energy densities that we have investigated. We have observed that the energy density in our water-tamped explosions levels off at about 25 kJ/gm. Attempts to drive the plasmas harder usually result in the formation of internal arcs that indicate nonuniform current density.

The pattern of roughly linear decrease in $\log_{10}(\sigma)$ vs $\log_{10}(V/V_0)$ at constant internal energy observed in the plots seems to hold until the internal energy reaches about

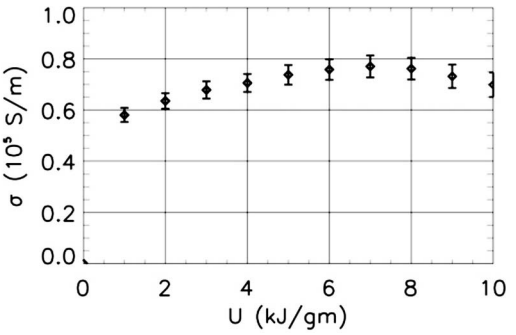


FIG. 5. Conductivity of a carbon fiber bundle in the prevaporization phase, at $V/V_0=0.62$. Error bars represent the standard error of the mean for 14 discharges.

25 kJ/gm, and the specific volume has increased by a factor of about 10. When the bank voltage is low, or the series resistance is high, so that the peak current never gets above 5 kA, a finite conductivity may persist for even larger expansion of the column, up to $V/V_0$ as much as 30 (Fig. 4) but the internal energy still appears to be limited to about 25 kJ/gm.

Figure 5 shows the development of the carbon conductivity in the early portion of the discharge, while the fiber is still in the solid state, for thirteen discharges. The initial resistance of the fiber is about 2 Ohms as expected, but the conductivity increases with heating until the internal energy has reached about 6 kJ/gm, in contrast to the behavior of metals where conductivity in the solid state decreases with temperature. This observation agrees with that in Refs. [16,17].

## VI. CONCLUSION

We have been able to produce nearly pure carbon plasmas over a range of densities from about 60% of solid density down to about 0.05 solid density, and to measure the electrical conductivity for these plasmas. The primary measurements are the current through, and voltage along, the plasma column, and streak images showing the time development of the column diameter. From these inputs, and with aid of a Lagrangian hydrodynamic model for the water surrounding the plasma, we deduce the specific volume, internal energy, and pressure in the plasma. The variation of conductivity with specific volume at constant internal energy is less pronounced than it is for some of the metals we have studied. In a future paper we will present contrasting data obtained in a similar manner for a number of metals.

## ACKNOWLEDGMENTS

We wish to acknowledge the contribution of A. D. Rakhel for suggesting the hydrodymanic approach to determination of pressures that was used in this work. This work was supported by the U. S. Army Research Laboratory, Aberdeen, MD.

[1] A. W. DeSilva and J. D. Katsouros, Phys. Rev. E **57**, 5945 (1998).
[2] A. W. DeSilva and A. D. Rakhel, Plasma Phys. **45**, 236 (2005).
[3] J. F. Benage, W. R. Shanahan, and M. S. Murillo, Phys. Rev. Lett. **83**, 2953 (1999).
[4] J. F. Benage, Phys. Plasmas **7**, 2040 (2000).
[5] G. S. Sarkisov, K. W. Struve, and D. H. McDaniel, Phys. Plasmas **12**, 052702 (2005).
[6] M. A. Berkovsky, D. Djordjevic, Yu. K. Kurilenkov, H. M. Milchberg, and M. M. Popovic, J. Phys. B **24**, 5043 (1991).
[7] H. Hess, A. Kloss, A. Rakhel, and H. Schneidenbach, Int. J. Thermophys. **26**, 1279 (2005).
[8] V. Recoules, J. Clerouin, P. Renaudin, P. Noiret, and G Zerah, J. Phys. A **36**, 6033 (2003).
[9] I. Krisch and H.-J. Kunze, Phys. Rev. E **58**, 6557 (1998).
[10] S. Saleem J. Haun, and H.-J. Kunze, Phys. Rev. E **64**, 056403 (2001).
[11] V. N. Korobenko, A. I. Savvatimski and R. Cheret, Int. J. Thermophys. **20**, 1247 (1999).
[12] J. Haun, H.-J. Kunze, S. Kosse, M. Schlanges, and R. Redmer, Phys. Rev. E **65**, 046407 (2002).
[13] S. P. Lyon and J. D. Johnson, Sesame: The Los Alamos National Laboratory Equation of State Database, LA-UR-92–3407, edited by S. P. Lyon and J. D. Johnson.
[14] M. N. Plooster, Phys. Fluids **13**, 02665 (1970).
[15] M. H. Rice and J. M. Walsh, J. Chem. Phys. **26**, 824 (1957).
[16] S. V. Lebedev and A. I. Savvatimski, Tepl. Vis Temp. **24**, 892 (1986).
[17] G. H. Kinchin,Proc. R. Soc. London, Ser. A **217**, 9 (1953).